Is There Icosahedral Ordering in Liquid and Undercooled Metals?

Andrea Di Cicco,* Angela Trapananti, and Silena Faggioni

Istituto Nazionale per la Fisica della Materia (INFM), INFN-LNF and Dipartimento di Fisica, Università degli Studi di Camerino, Via Madonna delle Carceri, I-62032 Camerino (MC), Italy

Adriano Filipponi

Istituto Nazionale per la Fisica della Materia (INFM)
and Dipartimento di Fisica, Università dell' Aquila, Via Vetoio, I-67010 Coppito, L'Aquila, Italy

The local structure of simple liquids is significantly different from that of corresponding crystalline systems. Signatures of fivefold local ordering have been previously found, but current knowledge is limited to pair distribution, leaving considerable uncertainty in the determination of the geometrical structure. New x-ray absorption experimental results on liquid and undercooled liquid copper, interpreted using an advanced data-analysis method based on multiple-scattering simulations, are shown to contain direct information on triplet correlations making feasible a reliable determination of the bond-angle distribution and fraction of nearly icosahedral configurations in liquids.

Even in simple liquids the short-range order may differ significantly from that of crystalline solids having similar densities and average interatomic spacing, as also inferred from the occurrence of deep undercooling in simple metals [1]. The possible existence of local icosahedral fivefold symmetry, forbidden by translational constraints in crystalline matter, was early proposed by Frank [2]. Pioneering structure investigations based on the Voronoi polyhedra analysis of random structures [3] and later works [4] have extensively addressed this question, but a comprehensive understanding is still lacking also because most experimental evidence is limited to pair-distribution information.

After the seminal works of the early times [1,2,5], a number of theoretical and experimental studies faced the problem of studying the local structure of close-packing liquids (see [3,4,6,7,8,9,10] and references therein). Suitable data-analysis techniques have been developed which are able to infer angular information in liquid matter, like the reverse Monte Carlo (RMC) [11] or the empirical potential structure refinement [12,13]. However, these methods have been applied to structural data containing information limited to the pair-distribution function $g_2(r)$, measuring the density fluctuation as a function of the interatomic distance. This limitation is intrinsic in the diffraction techniques sensitive to the "structure factor" $S(q)$, which is simply related to the $g_2(r)$ by Fourier transformation:

$$S(q) = 1 + \int_0^\infty dr 4\pi r^2 \rho [g_2(r) - 1] \frac{\sin(qr)}{qr}. \quad (1)$$

An alternative method which is very sensitive to short-range ordering and has a strong potential for applications to liquid matter [14] is the x-ray absorption spectroscopy (XAS).

In this technique, the photoelectron excited from a deep core level behaves as an effective short-range structural probe which interacts with the potential of the surrounding atoms generating scattering effects observed as oscillations in the absorption cross section.

The structural XAS signal $\chi(k)$ is defined as the relative oscillation of the x-ray absorption cross section above the edge under consideration as a function of the photoelectron wave-vector modulus $k = \sqrt{2m(E - E_e)}/\hbar$ (E_e being the threshold energy). Using third-generation synchrotron radiation sources, the structural XAS signal can be measured with very high accuracy even for samples under extreme conditions.

For a single component system the structural XAS signal is given by

$$\langle \chi(k) \rangle = \int_0^\infty dr 4\pi r^2 \rho g_2(r) \gamma^{(2)}(r, k) + \int dr_1 dr_2 d\theta 8\pi^2 r_1^2 r_2^2 \sin(\theta) \rho^2 g_3(r_1, r_2, \theta) \gamma^{(3)}(r_1, r_2, \theta, k) + \dots. \quad (2)$$

Because of the short-range nature of the n-body XAS $\gamma^{(n)}$ signals, the integrals are actually limited to a region of linear dimensions of the order of a few Å. The $\gamma^{(n)}(k)$ functions are usually regular oscillations as a function of k with a leading phase of kR_{path}, R_{path} being the length of the shortest path joining all of the atoms in the n-body configuration. Therefore, $R_{path} = 2r$ and

$R_{path} = r_1 + r_2 + r_3(r_1, r_2, \theta)$ for two-body and three-body terms, respectively, the latter corresponding obviously to oscillations of higher frequency in the XAS cross section as a function of k. As shown in Eq. (2), the dominant two-body term is usually accompanied by a detectable three-body high-frequency correction that

contains unique structural information on the short-range triplet distribution (g_3) in the system.

Recently, several advances in XAS data analysis have greatly increased the accuracy of the structural information obtained from experimental data. Major efforts have been devoted to the development of *ab initio* data-analysis methods based on multiple-scattering (MS) codes which allow us to obtain fast and accurate simulations of the $\gamma^{(n)}$ MS XAS n-body signals in wide r and k ranges [15,16]. It is clear that one of the most appealing features of XAS is its sensitivity to higher-order (and, in particular, three-body) distribution functions through the presence of multiple-scattering signals. This presence is well established for crystals and molecules [16] where characteristic signals associated with three-body configurations have been clearly identified and analyzed, extracting information on the geometry and correlated vibrations. The detailed analysis of three-body contributions in liquids needs additional improvements to the XAS data-analysis schemes. A successful method for quantitative analysis of highly disordered structures is the RMC refinement [11,17–19] that can be applied simultaneously to diffraction and XAS data, allowing the construction of a tridimensional model of the disordered system compatible with the observables under consideration.

In this Letter, we apply for the first time a RMC MS data-analysis method to XAS data of liquid and under-cooled liquid copper, for which accurate experiments have been performed at the European Synchrotron Radiation Facility third-generation synchrotron radiation source (BM29). The new method incorporates all of the advances included in the original XAS MS data-analysis program [15,16].

The samples were pellets constituted by dispersions of submicrometric Cu grains into a graphite matrix suitable for high-temperature measurements. Because of the low probability of nucleation events in such micrometric liquid droplets [1], the sample can be easily undercooled down to 100 K below the melting point as already observed for other metals and semiconductors (see [20,21,22] and references therein).

The XAS $k\chi(k)$ structural signal of liquid Cu measured at 1398 K (l-Cu) is compared with the two-body component of the RMC multiple-scattering simulation $k\gamma^{(2)}(k)$ in Fig. 1 (upper panel). The RMC simulation has been performed in a 864-atom cubic box of fixed density, considering both the XAS experimental data and the published $g_2(r)$ curve obtained by ND [23] which acts as a constraint for the long-range behavior. The RMC
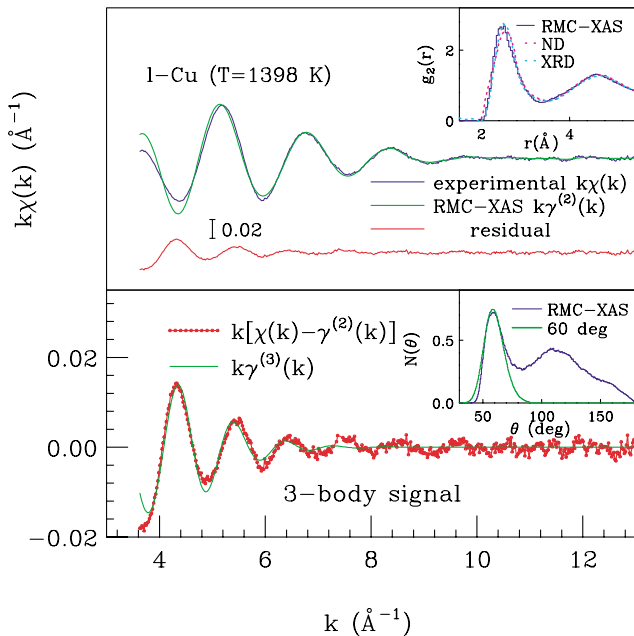

FIG. 1 (color online). XAS experimental data of liquid Cu at 1398 K (l-Cu) compared with the two-body component of the RMC multiple-scattering simulation (upper panel). The residual lower curve shows that the higher order terms have to be included to simulate the whole XAS spectrum. The inset shows the pair correlation function associated with the RMC simulation and previous determinations using neutron diffraction (ND) and x-ray (XRD) diffraction. The difference spectrum is compared in the lower panel with a XAS three-body signal calculated using a Gaussian three-body distribution for equilateral triangles. The full bond-angle $N(\theta)$ distribution resulting from the RMC simulation is compared with that of the equilateral triangles.
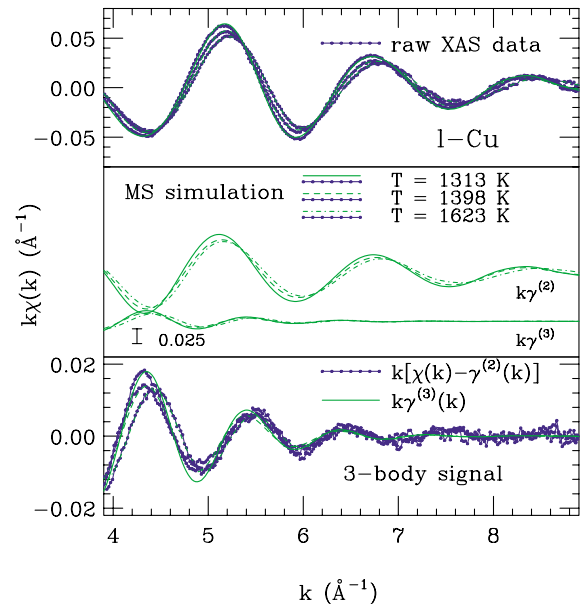

FIG. 2 (color online). XAS data of liquid and undercooled Cu at various temperatures compared with RMC MS simulations including three-body contributions (upper panel). The decomposition into two-body ($\gamma^{(2)}$) and three-body ($\gamma^{(3)}$) terms for each liquid is shown in the middle panel. XAS data after removal of the two-body contributions are compared with three-body MS simulations on the enhanced scale of the lower panel.
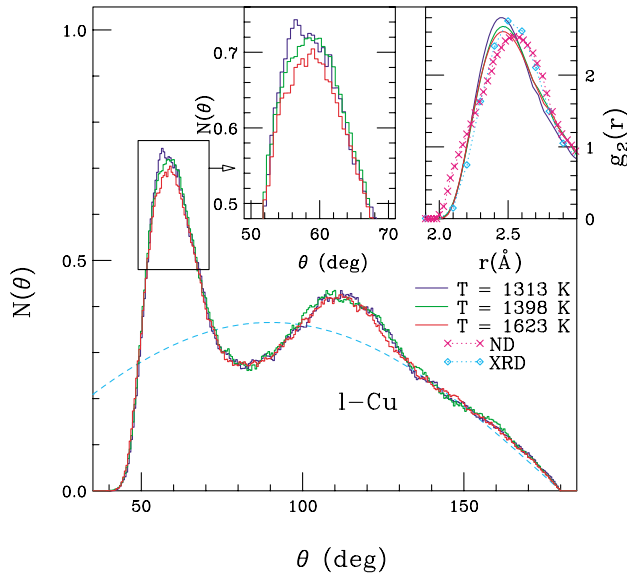
FIG. 3 (color). Bond-angle distribution $N(\theta)$ as determined by RMC simulations reproducing XAS data of liquid and undercooled Cu. The distribution shows a clear peak around 60° and another broad maximum at about 110°. The $N(\theta)$ corresponding to the uncorrelated limit is also shown (dashed line) for comparison. The number of nearly equilateral triangles increases lowering the temperature in the undercooling regime (see inset). The pair correlation functions of liquid and undercooled Cu measured by XAS are compared with previous ND and XRD diffraction determinations (see top-right figure).

curve reproduces almost exactly the shape of the ND [23] and XRD [24] $g_2(r)$ above about 4 Å while the first-neighbor peak is narrower and shifted to shorter distances [see also Fig. 3 (upper-right panel)]. The short-range shape of the RMC $g_2(r)$ is accurately reconstructed due to the unique sensitivity of the XAS signal. On the other hand, the high-frequency oscillation of the residual curve shows that the simple two-body $k\gamma^{(2)}$ contribution is not able to reproduce the entire experimental $k\chi(k)$ and this indicates that higher-order terms have to be included in the simulation. In a monoatomic close-packed liquid the smaller and mostly occurring three-body configuration is expected to be an equilateral triangle formed by first neighbors. The difference spectrum $k[\chi(k) - \gamma^{(2)}]$ is compared with a XAS three-body signal calculated using a Gaussian three-body distribution for equilateral triangles on an enhanced scale in the lower panel of Fig. 1. In fact, the main component of the XAS three-body signal is associated with the peak of the bond-angle $N(\theta)$ distribution associated with nearly equilateral triangular configurations, as shown in the inset of Fig. 1. The bond-angle distributions shown here are calculated counting the number of triangular configurations per atom up to a selected limiting distance, chosen in our case to enclose the first-neighbor peak ($R_{cut} = 2.98$ Å). The three-body MS signals have been therefore simulated accounting for the dominant terms associated with the nearly equilateral configurations.
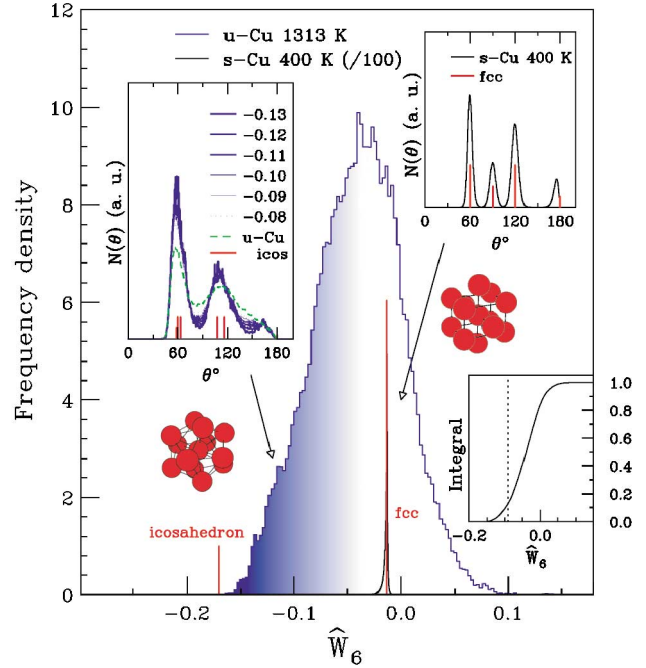
FIG. 4 (color). Histogram of the frequency density of the $\hat{W}_6$ cubic invariant monitoring the local geometry around each atom in undercooled liquid Cu. The histogram related to the fcc solid Cu, limited to a very narrow region around $-0.013\,161$ (value for a "perfect" fcc 13-atom cluster), is shown for comparison (scaled by a factor of 100). The $\hat{W}_6$ distribution is found to be very broad and includes a region (shaded area under the histogram) corresponding to distorted nearly icosahedral configurations as indicated by the typical angular distribution with peaks at 60° and 110° and a minimum at 90° (see the left inset).

The effect of the change of temperature on the XAS data of liquid Cu is shown in Fig. 2 (upper panel). At increasing temperatures ($T = 1623$ K) the $k\chi(k)$ signal amplitude and frequency are lowered. Instead, decreasing the temperature in a deep undercooled state the amplitude and frequency go in the opposite direction. The RMC two-body and three-body components are both affected by temperature as shown in the same figure (middle panel). The evolution of the three-body component as a function of temperature is reported in the lower part of the figure showing that both the two-body and three-body contributions are remarkably affected upon undercooling.

In Fig. 3 the bond-angle distributions $N(\theta)$ resulting from the RMC XAS refinement of liquid and undercooled Cu are presented. The cutoff distances for calculating the angle distributions have been scaled according to the liquid density ($R_{cut} = 2.97, 2.98, 3.0$ Å at $T = 1313$, 1398, and 1623 K respectively). The typical shape of the distribution contains a distinct peak around 60° associated with equilateral configurations and a second broad hump at about 110°. The peak at about 60° increases its intensity lowering the temperature in the undercooled state as shown in the left inset. The rest of the distribution is practically unchanged with temperature. This suggests

that the most important change of the local structure induced by cooling is the increase of the number of nearly equilateral configurations for an average given number of neighbors. At the same time, as shown in the upper-right inset, the first-neighbor two-body distribution is found to sharpen without a substantial change of the closest approach distance.

In order to get a deeper insight on the tridimensional average liquid structure we performed a detailed geometrical analysis with a set of bond orientational order parameters introduced by Steinhardt *et al.* [25] and used previously to study theoretical simulations of undercooled Lennard-Jones liquids [6,7,25]. The most sensitive indicator for icosahedral symmetry is the $\hat{W}_6$ cubic invariant, calculated using averages of spherical harmonics associated with the bond directions [6]. For an isolated 13-atom cluster, $\hat{W}_6 = -0.1698$ and $\hat{W}_6 = -0.013\,16$ for icosahedral and fcc (face centered cubic) structures, respectively. As we are considering an isotropic and homogeneous liquid and we are interested only in local symmetry we can calculate $\hat{W}_6$ for each atom of the RMC simulation at any equilibrium configuration, using the same cutoff distances defined above which enclose the first peak of the radial distribution.

In Fig. 4 we report the frequency density of the $\hat{W}_6$ cubic invariant calculated on about 100 configurations of the 864-atom box used for the RMC data analysis of undercooled Cu. The $\hat{W}_6$ distribution of the liquid is compared with that of a typical fcc crystalline solid (with vibrational amplitudes corresponding to Cu at about 400 K). In spite of the fact that the fcc angular distribution contains broadened peaks (see top-right inset), the corresponding $\hat{W}_6$ distribution is confined in a narrow region around the ideal fcc value ($\hat{W}_6 = -0.013\,16$) showing that this indicator is really very sensitive to the orientational symmetry. The $\hat{W}_6$ distribution of the liquid is found to be very broad and strongly asymmetric towards negative values extending down to the ideal value for a perfect icosahedral cluster. The $\hat{W}_6$ distribution of liquid Cu at higher temperatures has also been calculated and no significant changes of shape have been detected except for a slight shift toward higher $\hat{W}_6$ values.

The local geometry of clusters corresponding to lower $\hat{W}_6$ values approaches that of an icosahedron. This can be appreciated by visual inspection and can be verified looking at the $N(\theta)$ bond-angle distribution corresponding to selected $\hat{W}_6$ values. The bond-angle distributions $N(\theta)$ of clusters corresponding to selected regions of the $\hat{W}_6$ distribution are shown in the left inset of Fig. 4. The $N(\theta)$ corresponding to $\hat{W}_6$ values very near to the icosahedral limit ($\hat{W}_6 < -0.13$) shows a distinct high peak at 60° and a second peak around 110°, with a clear minimum at 90°, similarly to the ideal case shown by red ticks in the inset. These features obviously merge into the broadened $N(\theta)$ total distribution moving the upper $\hat{W}_6$ boundary but higher maxima at 60° and deeper minima at 90° are preserved up to intermediate values ($\hat{W}_6 \lesssim -0.09$). This upper limit corresponds to a broadening of about 10° around the ideal icosahedron values and can be taken as a reasonable borderline for nearly icosahedral configurations. Looking at the integral of the $\hat{W}_6$ distribution (right-lower inset) we can evaluate that the fraction of nearly icosahedral configurations in undercooled copper is around 10%.

*Electronic addresses: andrea.dicicco@unicam.it
http://gnxas.unicam.it/~dicicco

[1] D. Turnbull, J. Chem. Phys. **20**, 411 (1952).

[2] F. C. Frank, Proc. R. Soc. London A **215**, 43 (1952).

[3] J. L. Finney, Proc. R. Soc. London A **319**, 495 (1970).

[4] D. R. Nelson and F. Spaepen, Solid State Phys. **42**, 1 (1989).

[5] J. D. Bernal, Nature (London) **185**, 68 (1960).

[6] P. J. Steinhardt, D. R. Nelson, and M. Ronchetti, Phys. Rev. B **28**, 784 (1983).

[7] S. Nosé and F. Yonezawa, J. Chem. Phys. **84**, 1803 (1986).

[8] H. Jónsson and H. C. Andersen, Phys. Rev. Lett. **60**, 2295 (1988).

[9] H. Reichert, O. Klein, H. Dosch, M. Denk, W. Honkimäki, T. Lippmann, and G. Reiter, Nature (London) **408**, 839 (2000).

[10] T. Schenk, D. Holland-Moritz, V. Simonet, R. Bellissent, and D. M. Herlach, Phys. Rev. Lett. **89**, 075507 (2002).

[11] R. L. McGreevy, J. Phys. Condens. Matter **13**, R877 (2001).

[12] A. K. Soper, Chem. Phys. **202**, 295 (1996).

[13] A. K. Soper, Mol. Phys. **99**, 1503 (2001).

[14] A. Filipponi, J. Phys. Condens. Matter **13**, R23 (2001).

[15] A. Filipponi, A. Di Cicco, and C. R. Natoli, Phys. Rev. B **52**, 15 122 (1995).

[16] A. Filipponi and A. Di Cicco, Phys. Rev. B **52**, 15 135 (1995).

[17] R. L. McGreevy and L. Pusztai, Mol. Simul. **1**, 359 (1988).

[18] S. J. Gurman and R. L. McGreevy, J. Phys. Condens. Matter **2**, 9463 (1990).

[19] Y. Wang, K. Lu, and C. Li, Phys. Rev. Lett. **79**, 3664 (1997).

[20] A. Di Cicco, Phys. Rev. Lett. **81**, 2942 (1998).

[21] A. Filipponi, A. Di Cicco, and S. De Panfilis, Phys. Rev. Lett. **83**, 560 (1999).

[22] A. Filipponi and A. Di Cicco, Phys. Rev. B **51**, 12 322 (1995).

[23] O. J. Eder, E. Erdpresser, B. Kunsch, H. Stiller, and M. Suda, J. Phys. F **10**, 183 (1990).

[24] Y. Waseda, *The Structure of Non-Crystalline Materials* (McGraw-Hill, New York, 1980).

[25] P. J. Steinhardt, D. R. Nelson, and M. Ronchetti, Phys. Rev. Lett. **47**, 1297 (1981).